This is a preprint of an article published by Elsevier. The final version of Leire Meabe, Tan Vu Huynh, Daniele Mantione, Luca Porcarelli, Chunmei Li, Luke A. O'Dell, Haritz Sardon, Michel Armand, Maria Forsyth, David Mecerreyes, **UV-cross-linked poly(ethylene oxide carbonate) as free standing solid polymer electrolyte for lithium batteries**, *Electrochimica Acta*, (2019), 302, 414-421 is available at https://doi.org/10.1016/j.electacta.2019.02.058

UV-Cross-linked Poly(ethylene oxide carbonate) as Free Standing Solid Polymer Electrolyte for Lithium Batteries

Leire Meabe[1], Tan Vu Huynh[2], Daniele Mantione[1], Luca Porcarelli[1], Chunmei Li[3], Luke A. O'Dell[2], Haritz Sardon[1], Michel Armand[3], Maria Forsyth[2,4], David Mecerreyes[1,4*]

[1] *POLYMAT, University of the Basque Country UPV/EHU, Joxe Mari Korta Centre, Avda. Tolosa 72, 20018 Donostia-San Sebastián, Spain*

[2] *Institute for Frontier Materials (IFM), Deakin University, Waurn Ponds VIC 3216, Australia*

[3] *CIC Energigune, Alava Technology Park, Albert Einstein 4801510, MIÑANO Álava, Spain*

[4] *Ikerbasque, Basque Foundation for Science, E-48011 Bilbao, Spain*

E-mail address: david.mecerreyes@ehu.es

ABSTRACT

Aliphatic polycarbonates have emerged as promising polymer electrolytes due to their combination of moderate ionic conductivity and high lithium transference numbers. However, the mechanical properties of the aliphatic polycarbonates polymer electrolytes are usually weak due to the low molecular weight achieved and plasticization effect of the added lithium salt. In this article, we present a copolymer having poly(ethylene oxide) segments linked by carbonate groups with cross-linkable methacrylic pendant groups. Once the polymer and the lithium salt were mixed, the poly(ethylene oxide carbonate) was cross-linked by UV light producing a free standing solid polymer electrolyte (SPE). Different SPE formulations were designed by varying the LiTFSI concentration within the polymer matrix showing the highest ionic conductivity of $1.3 \cdot 10^{-3}$ S cm^{-1} and a lithium transference number of 0.59 at 70 °C. ^{7}Li solid-state NMR experiments were used to correlate the lithium cation environment and dynamics with ionic conductivity. At the same temperature the electrochemical stability window was analyzed, and a reasonable value of 4.9 V was achieved. The study was complemented by mechanical and thermal stability measurements. Finally, the optimized UV-cross-linked poly(ethylene oxide carbonate) was tested as electrolyte in lithium metal symmetric cell at 70 °C, showing low over-potential values and a stable solid electrolyte interphase layer.

Keywords: Polycarbonate, poly(ethylene oxide), Solid Polymer Electrolyte, free-standing polymer electrolyte, ionic conductivity, lithium conductivity, lithium transference number, ^{7}Li NMR, lithium battery

1. Introduction

Solid polymer electrolytes (SPEs) are desirable for the new generation of flexible and light-weight energy storage systems [1-3]. The main challenges of polymer electrolytes are to improve the poor electrochemical properties such as the limited ion conduction, poor lithium transference number and electrochemical window [4]. Among all matrixes proposed for SPEs, poly(ethylene oxide) (PEO) has been irreplaceable since the 1970s, due to its ability to solvate several salts, high thermal stability, mechanical properties, compatibility with metal electrodes and high values of ionic conductivity [5-7]. Different strategies have been developed to improve the performance of PEO-based SPEs: incorporation of different types of salt [5], chemical functionalization [8], single-ion conducting polymer electrolytes [9, 10], block copolymers [9, 11], introduction of inorganic nanoparticles or nanofillers [12, 13], and cross-linked PEO networks [14]. Nevertheless, the excellent electrochemical properties of PEO SPEs need to be further improved in particular with respect to the lithium transference number (aprox. 0.2) and electrochemical window (4.5 V). In recent years, research has been focused on exploring alternative chemistries for SPEs [15]; including, polycarbonates, polynitriles, polyalcohols or polyamines.

In particular, carbonate-containing aliphatic polymers have shown excellent electrochemical properties, which directly affect the final battery performance [16, 17]. Lithium transference number and electrochemical stability seem to be significantly enhanced with respect to PEO-based SPEs while maintaining similar ionic conductivity values. This has opened the possibility for room temperature operation solid state lithium batteries [18]. This improvement in electrochemical properties is normally attributed to the targeted coordination between the lithium cation and carbonyl group [19-21], which attributes in the dissociation of Li based salt. Nevertheless, generally, when low concentration of LiTFSI is included in the formulation of polycarbonate-SPE, it also acts as a plasticizer weakening its mechanical properties [22]. Therefore, if a true solid SPE film is desired, the mechanical stability of the polycarbonate SPE need to be improved. For this reason, several strategies have been proposed to surpass the poor mechanical stability of aliphatic polycarbonates such as introduction of cellulose nanofibers [23], Ti_2O nanoparticles [24], and cross-linking by γ irradiation [25].

In the present work, we present a cross-linkable poly(ethylene oxide carbonate) polymer precursor as a promising material to obtain free-standing SPE [26]. In the earlier work, the importance of ethylene oxide units in a polycarbonate backbone was showed as a way to improve the ionic conductivity of polycarbonates. However, the poor mechanical properties had to be improved in order to evaluate the performance in a battery. Therefore, the chemical structure of poly(ethylene oxide carbonate) was modified in this work by incorporating a methacrylic diol in the polycondensation synthesis. In a post-polymerization, the methacrylic functional polycarbonate was irradiated by ultraviolet light, obtaining a free-standing membrane. Different SPE formulations were designed with different LiTFSI concentrations, and the effect of the salt concentration on the lithium ionic conductivity, lithium transference number, lithium diffusion, environment and dynamics were studied. After analyzing the electrochemical window, the performance of the SPE (30 wt% LiTFSI) on a symmetric cell was investigated at 70 °C, showing low over-potential and stable solid electrolyte interphase layer values.

2. Experimental

2.1. Materials

Dry dimethyl carbonate (99+ %) (DMC) and 4-dimethylamino pyridine (DMAP) (99%) were purchased from Acros Organics. DMAP was also purchased by Fisher Scientific and was dried applying vacuum for 4 h at room temperature prior to use. Poly(ethylene glycol) (M_n 1,500 g mol^{-1}) was supplied by Fisher Scientific and was dried by azeotropic distillation (60 °C) in toluene for 8 h. Lithium bis(trifluoromethane)sulfonimide (LiTFSI) (99.9%) was supplied from Solvionic and the photoinitiator, 2-hydroxy-2-methylpropiophenone (DAROCUR), from Merck. Tetrahydrofuran (GPC grade) was obtained from Scharlab, acetonitrile (ACN) (HPLC grade), diethyl ether (Et_2O) (Extra Pure, SLR, Stabilised with BHT) and dichloromethane (DCM) (Certified AR for Analysis) from Fisher Scientific, toluene (HPLC grace) from Merck, and deuterated chloroform (99.8%) from Deutero GmbH.

2.2. Synthesis of diol with a pendant methacrylic group (bis-MPAmethracrylate)

Bis-MPA-methacrylic was synthesized in three steps following previously described work [27]. In the first step, a mixture of bisMPA (10.0 g, 1 equiv.), 2,2-dimethoxypropane (13,8 mL, 1.35 equiv.), and PTSA (0.7 g 5 %wt.) was stirred in 50 mL of acetone overnight at room temperature. To the reaction mixture 1 mL of a solution 1:1 NH4OH 30%:EtOH was added. The reaction mixture was evaporated to dryness and the residue was redissolved in 150 mL of DCM and rinsed three times with distilled water (20 mL), dried with Na_2SO_4. The solution was filtered and dried under vacuum. A white powdery residue was recovered 12 g (93%).

The second step consisted on the esterification of protected diol. To a solution of protected acid (3 g, 1.0 equiv.) in 150 mL of anhydrous DCM, 2-hydroxyethylmethacrylic (2.24 g, 0.9 equiv.) was added and the reaction mixture was kept 15 min in an ice bath. DIC (2.39 g, 1.1 equiv.) and DMAP (0.21 g, 0.1 equiv.) were then added and stirred for 48 h at room temperature, letting the ice melt slowly. After the reaction completion, the reaction mixture was filtered, to eliminate the urea salts precipitated during the reaction. The product containing filtrate was diluted with extra 250 mL of DCM and rinsed 3 times with 100 mL of water. The organic phase was dried over Na_2SO_4, and concentrated. The concentrated product was loaded onto a silica gel column and purified by flash column chromatography using a mixture of hexanes/EtOAc (7:3 v/v), Rf ¼ 0.69, to give 6.65 g (84%) as yellowish liquid.

The third and last step is the deprotection of the acetonide moiety. 1.9 g of the protected diol methacrylic were added to 400 mL of MeOH, together with 9.5 g of DOWEX® 50W-X8, and let stirred overnight at room temperature. Filtration of the suspension and drying under vacuum of the solvent lead the diol methacrylic as pure compound in quantitative yield (~100%). Rf ¼ 0.05 hexanes/ EtOAc (7:3 v/v).

2.3. Synthesis cross-linkable poly(ethylene oxide$_{34}$ carbonate) with 10 wt% MA: PEO$_{34}$-PC 10 wt% MA

The synthesis of UV-curable polycarbonate was performed using the same synthetic process as previously described [28]. The following amounts of reactants were used in the synthesis: DMC (1.5 mL, 17.84 mmol, 8 eq.), diols (1 eq.): PEG1500 (2 g, 1.33 mmol, 0.6 eq), and methacrylic diol (MA) (0.22 g, 0.9 mmol, 0.4 eq), and DMAP (2.7 mg, 0.0223 mmol, 0.01 eq.). 10 wt% of UV curable monomer respect to the overall diol

used was incorporated. It was necessary to add few ppm of hydroquinone in order to prevent the polymerization from the double bonds during the polycondensation steps. During the first 7 hours of the polycondensation, the reaction was maintained at 130 °C and later, the temperature was increased up to 170 °C and high vacuum was applied overnight. Once the reaction was stopped, the polymer was dissolved in dichloromethane and powdered in cold diethyl ether. The disappearance of the monomers was confirmed by ^{1}H NMR. Moreover, the double bonds of the methacrylic diol could be determined by ^{1}H NMR. In the final polymer, 23 mol % of MA was achieved. The polymer was characterized by ^{1}H NMR ($CDCl_3$, 400 MHz): δ= 6.13, 5.57 (s, C=C***H***$_2$, 2H), 4.45-4.29 (s (OCOOC***H***$_2$C, 4H), 4.28 (t, OCOOC***H***$_2$CH$_2$, 4H), 3.82 (t, OCOC***H***$_2$C***H***$_2$OCO, 4H) 3.71 (t, OCOOCH$_2$C***H***$_2$, 4H), 3.64 (s, OCOCH$_2$CH$_2$OC**H**$_2$, 128H), 1.95 (s, OCOOCH$_2$CC***H***$_3$, 3H), 1.25 (s, H$_2$C=CC***H***$_3$, 3H). The yield of the polymerization was determined by gravimetry (yield = 70 %).

2.4. Preparation of ultraviolet cross-linked polymer electrolytes: PEO_{34}-PC 10 wt% MA with LiTFSI

For the preparation of ultraviolet cross-linked SPEs, the polymer, the salt (LiTFSI), and the UV initiator (2-hydroxy-2-methylpropiophenone (1 wt% respect to the initial MA amount)), were dissolved in ACN. In each SPE a specific LiTFSI concentration was added: 0 wt%, 15 wt%, 20 wt%, 25 wt% 30 wt%, 40 wt%, 50 wt% and 80 wt%. Once the solutions were stirred during 10 minutes, they were cast onto a silicon mold. The solvent was removed at room temperature and later by applying high vacuum. Finally, the films were passed 3 times from a xenon arc lamp (Helios Italquartz, 45 mW cm^{-2}). Before performing any electrochemical characterization, the SPEs were first dried under vacuum at room temperature during 24 h, and after, it was completed in an oven inside an argon-filled glove box, increasing the temperature up to 60 °C and applying vacuum for 24 h.

2.5. Characterization methods

^{1}H and ^{13}C Nuclear Magnetic Resonance (NMR) spectra were recorded on Bruker spectrometers at 400 MHz at room temperature, using deuterated chloroform. Diffusion measurements were carried out on a 300 MHz Bruker Advance III spectrometer with a Diff50 pulsed field gradient probe and a stimulated echo pulse sequence. Relaxation measurements were carried out on the same hardware with a saturation recovery pulse sequence. Attenuated Total Reflectance Fourier Transform Infrared Spectroscopy (ATR-FTIR) measurements were conducted on a Bruker ALPHA Spectrometer.

Molar mass distributions of polymers were measured by size exclusion chromatography (SEC). Samples were diluted in THF (GPC grade) to a concentration of approximately 5 mg mL^{-1} and filtered through a 0.45 mm nylon filter. The SEC set up consisted of a pump (LC-20A, Shimadzu), an autosampler (Waters 717), a differential refractometer (Waters 2410) and three columns in series (Styragel HR2, HR4, and HR6 with pore sizes ranging from 10^2 to 10^6 Å). Chromatograms were obtained in THF (GPC grade) at 35 °C using a flow rate of 1 mL min^{-1}. The equipment was calibrated using narrow polystyrene standards ranging from 595 to 3.95 · 10−6 g mol^{-1} (5^{th} order universal calibration).

Differential Scanning Calorimetry (DSC) was performed on a DSC Q2000 differential calorimeter (TA Instruments). All the experiments were performed under ultrapure nitrogen flow. Samples of 5 mg were used. Measurements were performed by placing the samples in sealed aluminium pans. The samples were first heated at a rate of 20 K min^{-1}, from 25 °C to 100 °C and they were left 3 min at 100 °C to avoid the influence of thermal history, in order to be able to compare the crystallization/melting temperature afterward. Subsequently, the sample was cooled down to -70 °C at a rate of 20 K min^{-1} and then heated to 100 °C at 20 K min^{-1} after waiting at -70 °C during 3 min.

The mechanical properties were analyzed by rheological measurements using an AR-G2 rheometer (TA Instruments) with parallel geometric plates (diameter 12 mm). Angular frequency sweeps were performed in the range of $6^2 < \omega < 6^{-2}$ rad s^{-1} at different temperatures (30 °C, 70 °C and 100 °C) in the linear viscoelastic regime. The time required for a frequency sweep was 5 min. Each measurement was repeated at least two times observing a good reproducibility. On the other hand, the thermogravimetry analysis was performed at N_2 atmosphere at 10 K min^{-1} in Q500 TA Instruments.

All the electrochemical characterization was carried out in a VMP3 (Biologic, Claix, France) potentiostat. Ionic conductivity (σ) of the polymer electrolytes was determined by AC impedance spectroscopy over the frequency range from 100 mHz to 1 MHz with an amplitude of 10 mV. The conductivities were analyzed in a temperature range down from 100 °C to 25 °C. All cells were assembled in an argon-filled glove box (M-Braun). The solid polymer electrolytes were closed in CR2032, sandwiched between two stainless steel (SS) electrodes. In all the cases the average surface area of the electrode is 2.01 cm^2. Lithium transference number was calculated based on Bruce and Vincent method at 70 °C [29]. The electrolytes were sandwiched between two lithium disks in CR2032. Before the analysis, the cells were left to stabilize at 70 °C for 24 h. The lithium ionic conductivity was calculated by multiplying the total ionic conductivity with lithium transference number at 70 °C [30]. Electrochemical stability window was determined by applying cyclic voltammetry (CV) of the polymer electrolyte at 70 °C. The anodic limit was evaluated between open circuit potential (OCV) and 6 V *vs.* Li^+/Li at a constant rate of 0.5 mV s^{-1}. On the other hand, the cathodic scan was determined between OCV and -0.5 V vs. Li^+/Li using the same scan rate. Before performing the experiment, the electrolytes were left stabilizing for 24 h at 70 °C.

Symmetric cell test was performed at 70 °C after stabilization at that temperature during 48 h. The SPE was sandwiched between two lithium metallic dicks. The effect of change of current density on the over potential and solid electrolyte interphase layer is analyzed.

3. Results and discussion.

3.1. Synthesis and physicochemical characterization of cross-linked polycarbonate: PEO_{34}-PC 10 wt% MA.

Based our previous work, we observed that both structures (ethylene oxide and carbonyl groups) play an important role in the electrochemical behaviour [26]. Specially, the polycarbonate with 34 ethylene oxide units gave reasonable improved values. However, the low molecular weight of the polymer and the plasticizing ability of LiTFSI lead in poor mechanical properties. Therefore, in this work, we have incorporated cross-linkable methacrylic groups in order to developed a free standing SPE, based on

polycarbonate containing 34 ethylene oxide units, **Scheme 1a**. Poly(ethylene glycol) (M_n= 1500 g mol^{-1}) and methacrylic based diol (MA) were copolymerized using dimethyl carbonate via polycondensation. Different copolymers were synthesized having 5, 10 and 20 wt% of methacrylic diol respect to the overall diol introduced to the formulation, which are named as PEO_{34}-PC 5 wt% MA, PEO_{34}-PC 10 wt% MA and PEO_{34}-PC 20 wt% MA respectively. The polymerization was organocatalysed by DMAP, in a two steps reaction, where high temperature and high vacuum are necessary: 1st step: 130 °C, 7 h and 2nd step: 170 °C and high vacuum, overnight. The chemical structures of the polycarbonates were confirmed by ^{1}H NMR, which is shown in **Figure S1,** indicating the presence of methacrylic pendant units**.** The molar mass of the methacrylic functional poly(ethylene oxide carbonate) before cross-linking was measured by GPC, showing a M_n value of 20,000 g mol^{-1}. The functional methacrylic poly(ethylene oxide carbonate) was further cross-linked by ultraviolet light in the presence of a photoinitiator, **Scheme 1b**. The polymer, targeted LiTFSI amount, and the photoinitiator were dissolved in ACN. Once the solvent was evaporated, the dry films were exposed under ultraviolet light. After UV treatment a free standing solid membrane was obtained as shown in the picture, **Scheme 1b**.

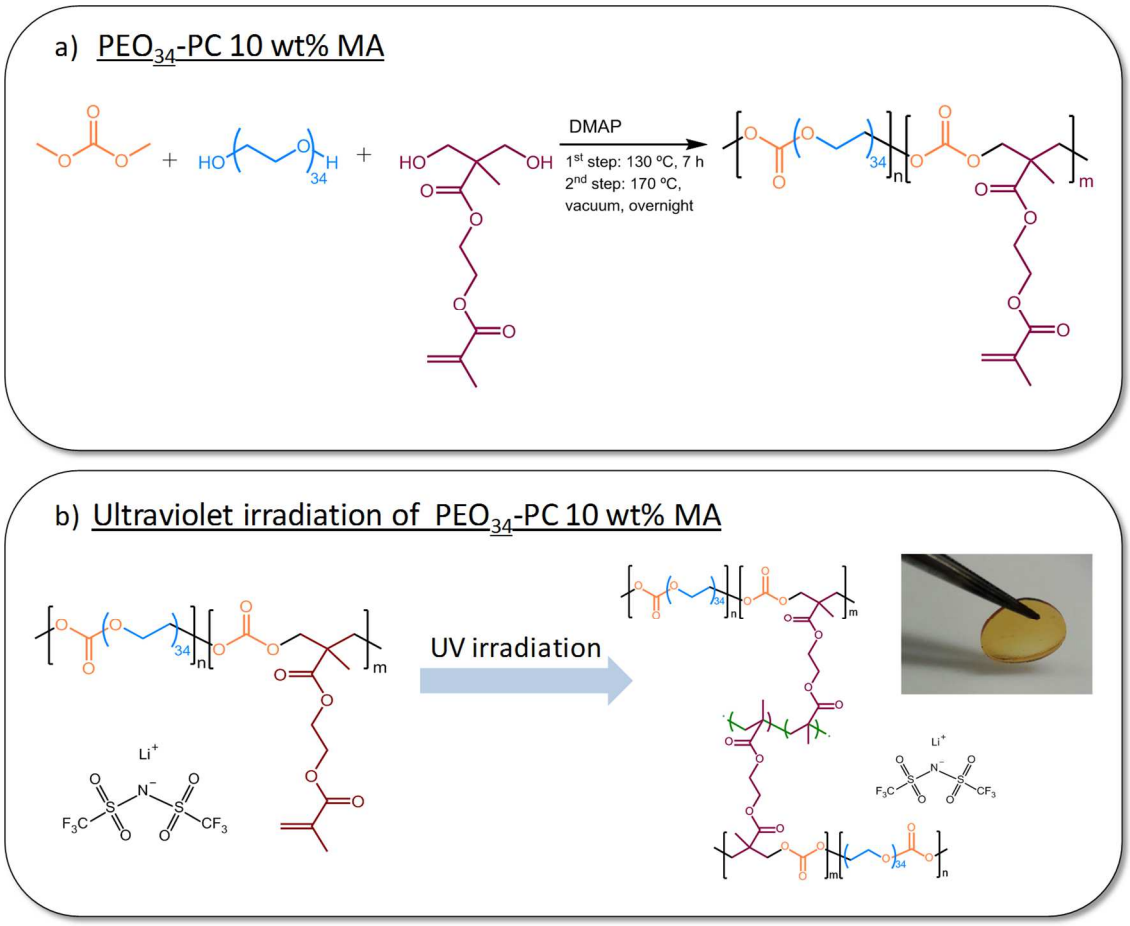

Scheme 1. a) Synthetic route of cross-linkable methacrylic functional PEO_{34}-PC b) Schematic representation of the ultraviolet curing of the SPEs.

After ultraviolet treatment, the PEO_{34}-PC copolymer became insoluble in common organic solvents. Furthermore, FTIR-ATR was used to investigate the chemical nature of the cross-linking reaction. It has to be mentioned that this analysis was carried out before the addition of LiTFSI. FTIR-ATR analysis of PEO_{34}-PC 10 wt% MA, **Figure 1a**, confirmed the disappearance of double bonds, in 1717 cm^{-1} and, besides, new bands were described; 1680 cm^{-1}, 720 cm^{-1}, and 700 cm^{-1}, corroborating the formation of the cross-linked network due to the reactivity of the methacrylic units. Additionally, we performed DSC analysis to study the effect of the cross-linked network on the thermal properties of PEO_{34}-PC 10 wt% MA, as it can be observed in the supporting information, **Figure S2**. The glass transition of the non-cross-linked to the cross-linked network was compared; the glass transition of the non cross-linked polymer was found to be -55 °C, whereas

the glass transition of cross-linked polymer electrolyte was -45 °C. Besides, the enthalpy of melting is maintained, nonetheless, a different crystal formation can be observed from the DSC traces.

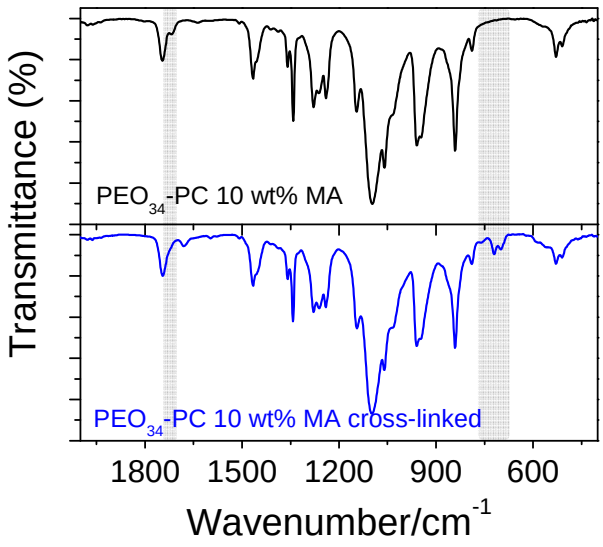

Figure 1. FTIR-ATR analysis of PEO_{34}-PC 10 wt% MA before and after cross-linking.

The cross-linked architecture of PEO_{34}-PC 10 wt% MA containing 30 wt% of LiTFSI was confirmed by the study of the viscoelastic properties through AR-G2 rheometer, in the temperature range between 30 and 100 °C. **Figure 2** depicts the double-logarithmic plots of G' and G" *vs.* angular frequency of PEO_{34}-PC 10 wt% MA containing 30 wt% of LiTFSI. As can be observed from the figure, the storage modulus of the material is above the loss modulus at all temperatures, which means that the polymer is in the rubbery plateau region, confirming a three-dimensional network. Nevertheless, G' and G'' values depends on frequency and temperature, which could be argued with the remaining methacrylic groups after the post-polymerization, when LiTFSI is added in the system. All in all, the rheological experiments confirmed the solid nature of the free standing SPE membrane even at high temperatures. Additionally, the thermal stability was studied by thermogravimetic analysis, **Figure S3**. The onset temperature (T_{onset}) for PEO_{34}-PC 10 wt% MA containing 30 wt% of LiTFSI was found to be 275 °C.

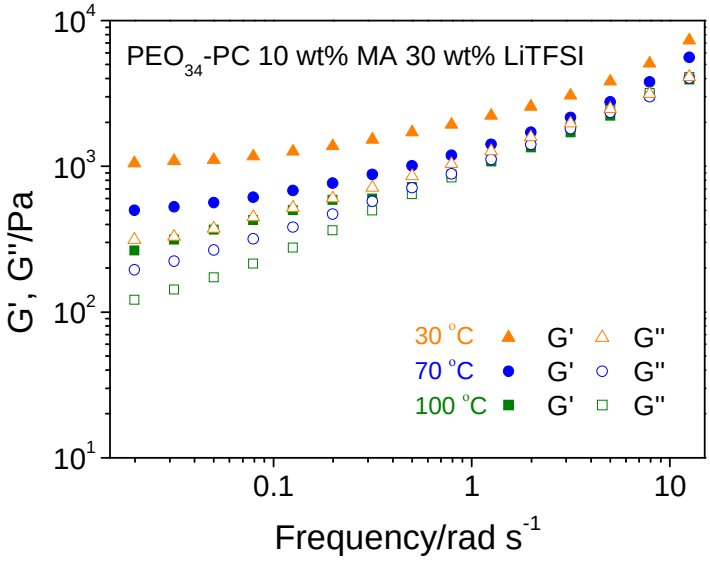

Figure 2. Elastic and viscous modulus (G' and G'', respectively) of cross-linked PEO_{34}-PC 10 wt% MA containing 30 wt% LiTFSI at different temperatures (30 °C, 70 °C and 100 °C).

3.2. Electrochemical characterization of the cross-linked PEO-PC polycarbonate SPEs

First, the effect of methacrylic content in the copolymer, which should affect the cross-linking density of SPEs on ionic conductivity, was evaluated. Thus, PEO_{34}-PC copolymers with 5, 10 and 20 wt% of methacrylic monomer and 30 wt% of LiTFSI were investigated. Even though 5 wt % methacrylic monomer gives slightly higher ionic conductivity ($3.6 \cdot 10^{-5}$ S cm^{-1} at room temperature), 10 wt% of methacrylic diol was observed to be the minimum amount to succeed in obtaining a free standing SPE. Besides, the ionic conductivity decreases from $3.2 \cdot 10^{-5}$ S cm^{-1} with 10 wt% MA to $9.4 \cdot 10^{-6}$ S cm^{-1} with the addition of 20 wt% of MA at room temperature. Therefore, the polymer with 10 wt% of methacrylic monomer was chosen for further studies.

Second, electrochemical properties were investigated varying the LiTFSI concentrations in the polymer with 10 wt% methacrylic diol, with the aim of determining the optimum composition for testing in lithium-based battery. Initially, the salt concentration was varied from 15 wt% to 80 wt% (**Figure 3a**). The highest conductivity value of $3.2 \cdot 10^{-5}$ S cm^{-1} at room temperature is obtained with 30 wt% of LiTFSI, equivalent to an O:Li mole ratio of 1:16. We have to remark, that this value is not compromised by the cross-linked

network, compared with $3.7 \cdot 10^{-5}$ S cm^{-1} for the non-cross-linked PEO_{34}-PC at ambient temperature, that we previously reported [26]. Besides, the ionic conductivity showed at 70 °C is $1.3 \cdot 10^{-3}$ S cm^{-1}. The trend with cross-linked SPEs is comparable to the case of non-cross-linked ones; when the salt concentration is lower than 30 wt% of LiTFSI, the crystallinity is pronounced, as shown in DSC analysis, **Figure 3b**, and these crystalline domains restrict the ion conduction. Therefore, the ion movement is increased while the crystallinity is suppressed, the case of 30 wt% of LiTFSI. Besides, if the salt concentration is increased more than 30 wt%, the ionic conductivity decreases due to the increase on the glass transition temperature. With the high amount of LiTFSI, 80 wt%, the glass transition increases more than 10 °C respect to 30 wt% of LiTFSI, which provokes that the ionic conductivity decreases one order of magnitude. This ionic conductivity behaviour has more similarity to PEO based SPE rather than polycarbonate SPE. In the later case, a higher salt concentration, generally increases the ionic conductivity [22].

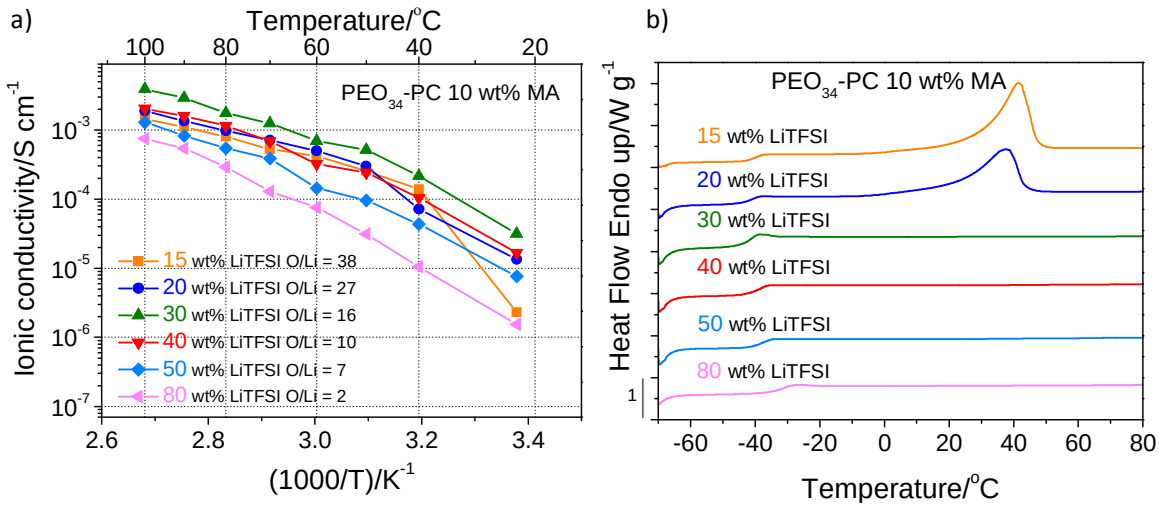

Figure 3. Ionic conductivities and DSC measurements of cross-linked PEO_{34}-PC 10 wt% MA. a) The effect of LiTFSI concentration on ionic conductivity. b) DSC traces of corresponding PEO_{34}-PC 10 wt% MA with different LiTFSI concentrations during the second heating scan at 20 K min^{-1}.

Then, we measured the lithium transference number at 70 °C using the Bruce and Vincent method [29] in order to see if carbonate group is involved in any electrochemical property. The LiTFSI concentration was varied between 15 wt% to 50 wt% to study the effect of salt concentration on the transference number, the results are shown in **Figure 4**. The lithium transference number varies with the LiTFSI composition, showing

the highest value of 0.59 for the SPE containing 30 wt% of LiTFSI (experimental results can be seen in the supporting information, **Figure S4**). This value compares favourably with PEO-based SPE with 30 wt% LiTFSI, which is close to 0.17. This clearly shows the previous observations of other authors on the favourable effect of carbonyl groups on the lithium transference number [19]; the carbonyl group help to dissociate the LiTFSI, leading to favourable lithium mobility. This optimum value of 30 wt% LiTFSI can be discussed with the ideal balance of Li cation and the amount of carbonyl groups on the system: i) a lower concentration of salt than 30 wt% LiTFSI, can lead in free carbonyl groups and also, in lower cations in the systems, and ii) a system with higher LiTFSI concentration, not all the Li cations can be coordinated by carbonyl moieties and they will coordinate with ethylene oxide units. Therefore, the lithium transference number will decrease.

Using this lithium transference values and the total ionic conductivity, we could calculate the ionic conductivity of the lithium cation conductivity at 70 °C, **Figure 4**. As expected, SPE containing 30 wt% of LiTFSI presents the highest lithium ionic conductivity among all the samples, $7.4 \cdot 10^{-4}$ S cm^{-1}, hence this composition was further investigated in symmetric cells.

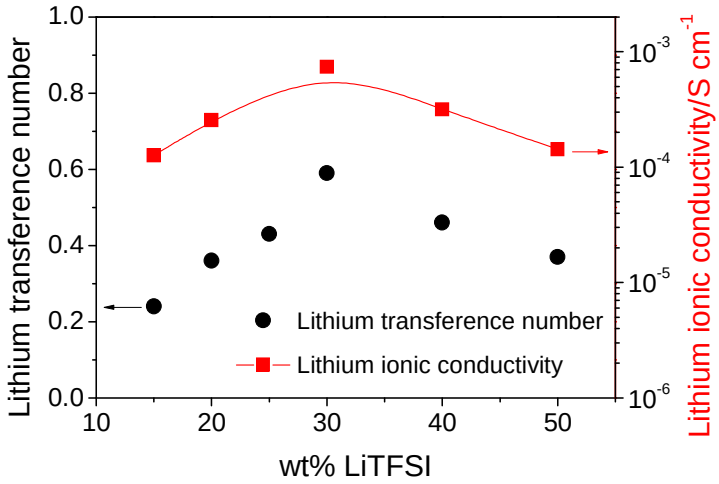

Figure 4. Lithium transference number in black (●) and lithium ionic conductivity in red (■) of different cross-linked PEO_{34}-PC 10 wt% MA membranes at 70 °C.

^{7}Li solid-state NMR experiments were used to investigate the lithium cation environment and dynamics, and their dependence on the LiTFSI salt content. Pulsed field gradient diffusion measurements were used to measure the ^{7}Li self-diffusion coefficients, **Figure 5**. These data show a clear trend of decreasing lithium cation diffusion coefficients as the salt content is increased. Faster timescale, shorter-range dynamics were also probed via ^{7}Li T_1 relaxation measurements, which were fitted using the same method as outlined in our previous publication [26]. The resulting parameters are shown in **Table 1**, again as a function of the LiTFSI content. The quadrupolar coupling constant C_Q gives an insight into the symmetry of the Li^+ coordination environment (via the local electric field gradient), and the decreasing value as LiTFSI content increases reflects the Li^+ environment becoming slightly more symmetric on average. Alongside this trend, the correlation time τ_c increases while the activation energy for this motional process decreases with increasing LiTFSI concentration. The former implies a decrease in the local dynamics around the Li^+ while the latter implies that the local dynamics become more energetically favourable. This apparent contradiction would be best explained by a change in the local coordination environment as the LiTFSI content increases, which is also what the changing C_Q values imply. This is most likely the effect of the competing coordination of the Li^+ by the TFSI anions and the ether oxygens of the polymer. These results can lead to understand why lithium ionic conductivity is decreased with the increase of LiTFSI concentration. Different environments can affect on a higher/lower lithium ionic conductivity when LiTFSI concentration is varied.

Table 1. ^{7}Li quadrupolar coupling constants (C_Q), motional correlation times (τ_c) and activation energies (E_A) extracted from the fitting of the NMR T_1 relaxation times.

Samples	C_Q (kHz)	τ_c (ns) at 343.15 K	E_A (kJ mol^{-1})
20 wt% LiTFSI	26.59±0.49	2.17±0.04	28.83±0.53
30 wt% LiTFSI	25.64±0.47	2.53±0.05	26.02±0.48
40 wt% LiTFSI	24.83±0.46	2.52±0.05	26.90±0.49
50 wt% LiTFSI	23.14±0.43	4.25±0.08	20.24±0.37

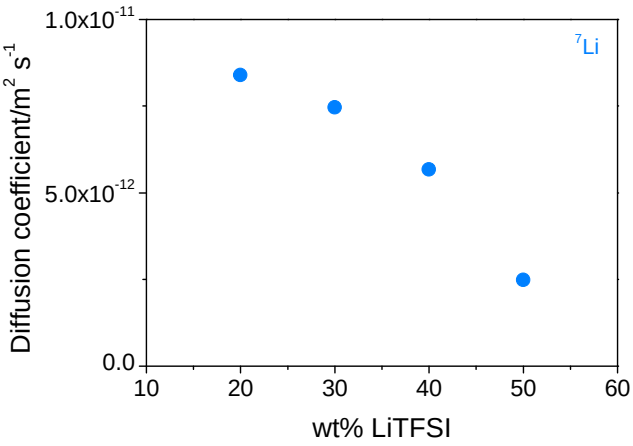

Figure 5. ^{7}Li diffusion coefficients as a function of wt% LiTFSI measured using pulsed field gradient NMR at 70 °C.

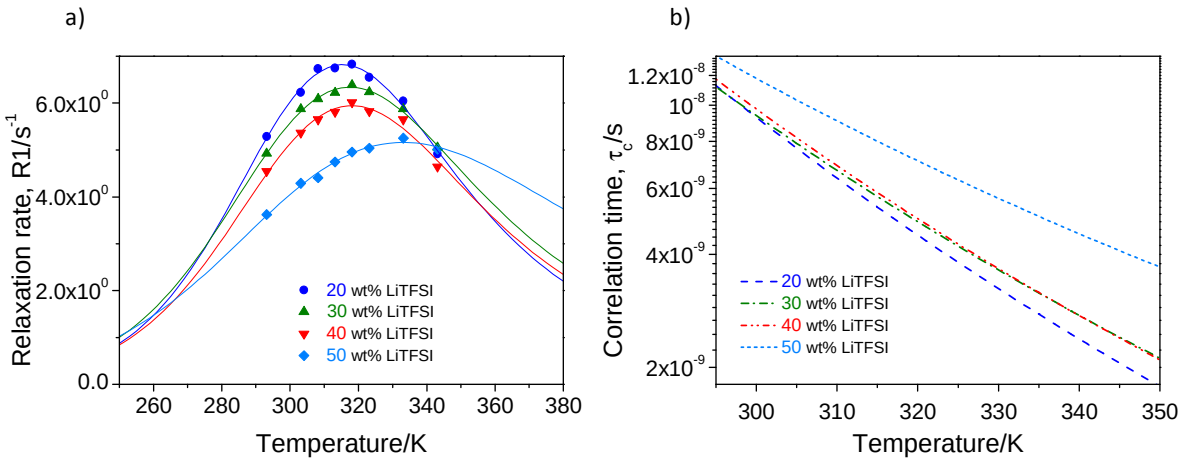

Figure 6. a) Fits of the ^{7}Li T_1 relaxation data and b) temperature dependent ^{7}Li motional correlation times.

The electrochemical stability of the SPE based on PEO_{34}-PC 10 wt% MA containing 30 wt% of LiTFSI was investigated at a scan rate of 0.5 mV s^{-1} at 70 ºC, **Figure 7**. The anodic limit of the SPE was 4.9 V *vs.* Li^{+}/Li. During the cathodic scan, we observe a peak corresponding to the lithium plating process between 0 and -0.5 V *vs.* Li^{+}/Li and the peak corresponding to the reverse process – stripping of lithium – between 0 and 0.6 V *vs.* Li^{+}/Li.

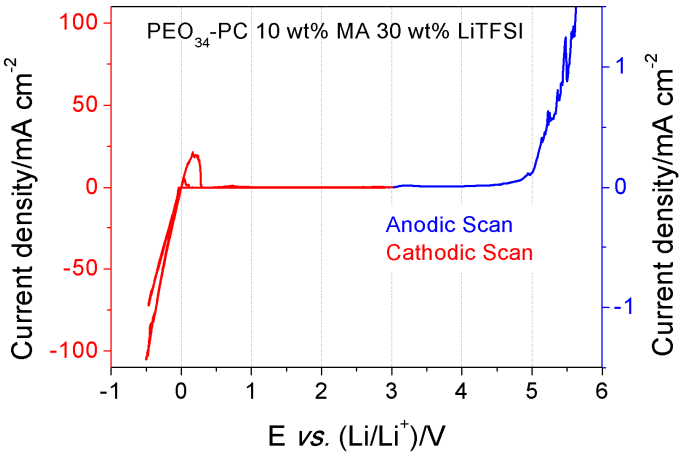

Figure 7. Electrochemical stability of cross-linked PEO_{34}-PC 10 wt% MA containing 30 wt% LiTFSI. Cyclic voltammetry was carried out at 0.5 mV s^{-1} at 70 °C.

3.3. Electrochemical behaviour Li cell: PEO_{34}-PC 10 wt% MA 30 wt% LiTFSI

To further confirm the viability of the SPE in Li-based cells, lithium symmetric cells were assembled and cycled at different current densities at 70 °C, **Figure 8**. At 0.1 mA cm^{-2}, the cell over-potential is around 10-50 mV which is comparable with state-of-the-art polymer electrolytes commonly used in the Li-based symmetric cells [31]. Increasing the applied current density from 0.1 mA cm^{-2} to 0.5 mA cm^{-2}, the overpotential of the symmetric cell also increased to 200 mV. The increased cell over-potential is due to the kinetics limitation of the Li charge transfer in the SPE and/or the solid electrolyte interphase (SEI) layer of Li/electrolyte. The impedance spectroscopy showed no significant change on the resistance of the SEI (corresponds to the first semicircle at high frequencies) with the variation on current density at the Li stripping/plating process. Besides, the second semicircle that is observed in Nyquist plot at low frequencies can be related to the mass transfer process.

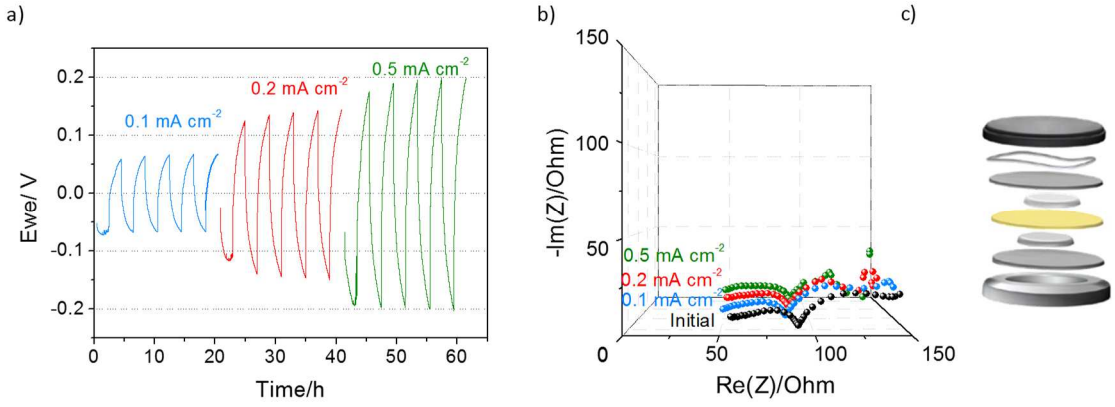

Figure 8. Lithium symmetric cell of cross-linked PEO_{34}-PC 10 wt% MA containing 30 wt% LiTFSI. a) The evolution of overpotential with different current densities. b) Nyquist plot after applying different current densities. c) Scheme of symmetric cell assembly.

4. Conclusions

Free-standing solid polymer electrolytes were successfully developed by incorporating 10 wt% of methacrylic monomer into the poly(ethylene oxide carbonate) main chain. These membranes showed promising electrochemical values, such as high lithium ionic conductivity and transference number, $7.4 \cdot 10^{-4}$ S cm^{-1} and 0.59 respectively, at 70 °C with 30 wt% of LiTFSI. ^{7}Li NMR showed a change on coordination environment while LiTFSI concentration is varied, which can be understood the ionic conductivity trend. The test of this SPE formulation into a lithium symmetric cell proved the stability of the membrane against lithium metal. Moreover, the wide electrochemical stability opens opportunities to employ the membrane in different Lithium battery technologies.

5. Acknowledgements

We are grateful to the financial support of the European Research Council by Starting Grant Innovative Polymers for Energy Storage (iPes) 306250 and the Basque Government through ETORTEK Energigune 2013 and IT 999-16. Leire Meabe thanks Spanish Ministry of Education, Culture and Sport for the predoctoral FPU fellowship received to carry out this work. The authors would like to thank the European Commission for their financial support through the project SUSPOL-EJD 642671 and the Gobierno

Vasco/Eusko Jaurlaritza (IT 999-16). The authors thank for technical and human support provided by SGIker of UPV/EHU for the NMR facilities of Gipuzkoa campus.

6. References

[1] M. Armand, J.M. Tarascon, Building better batteries, Nature, 451 (2008) 652.
[2] V. Di Noto, S. Lavina, G.A. Giffin, E. Negro, B. Scrosati, Polymer electrolytes: Present, past and future, Electrochimica Acta, 57 (2011) 4-13.
[3] B. Scrosati, J. Garche, Lithium batteries: Status, prospects and future, Journal of Power Sources, 195 (2010) 2419-2430.
[4] E. Strauss, S. Menkin, D. Golodnitsky, On the way to high-conductivity single lithium-ion conductors, Journal of Solid State Electrochemistry, 21 (2017) 1879-1905.
[5] M. Armand, Polymer solid electrolytes - an overview, Solid State Ionics, 9 (1983) 745-754.
[6] M. Armand, The history of polymer electrolytes, Solid State Ionics, 69 (1994) 309-319.
[7] M.B. Armand, Polymer Electrolytes, Annual Review of Materials Science, 16 (1986) 245-261.
[8] D. Brandell, P. Priimägi, H. Kasemägi, A. Aabloo, Branched polyethylene/poly(ethylene oxide) as a host matrix for Li-ion battery electrolytes: A molecular dynamics study, Electrochimica Acta, 57 (2011) 228-236.
[9] R. Bouchet, S. Maria, R. Meziane, A. Aboulaich, L. Lienafa, J.-P. Bonnet, T.N.T. Phan, D. Bertin, D. Gigmes, D. Devaux, R. Denoyel, M. Armand, Single-ion BAB triblock copolymers as highly efficient electrolytes for lithium-metal batteries, Nat Mater, 12 (2013) 452-457.
[10] L. Porcarelli, A.S. Shaplov, M. Salsamendi, J.R. Nair, Y.S. Vygodskii, D. Mecerreyes, C. Gerbaldi, Single-Ion Block Copoly(ionic liquid)s as Electrolytes for All-Solid State Lithium Batteries, ACS Applied Materials & Interfaces, 8 (2016) 10350-10359.
[11] A. Panday, S. Mullin, E.D. Gomez, N. Wanakule, V.L. Chen, A. Hexemer, J. Pople, N.P. Balsara, Effect of molecular weight and salt concentration on conductivity of block copolymer electrolytes, Macromolecules, 42 (2009) 4632-4637.
[12] S. Chung, Y. Wang, L. Persi, F. Croce, S. Greenbaum, B. Scrosati, E. Plichta, Enhancement of ion transport in polymer electrolytes by addition of nanoscale inorganic oxides, Journal of power sources, 97 (2001) 644-648.
[13] F. Croce, L. Persi, B. Scrosati, F. Serraino-Fiory, E. Plichta, M. Hendrickson, Role of the ceramic fillers in enhancing the transport properties of composite polymer electrolytes, Electrochimica Acta, 46 (2001) 2457-2461.
[14] A. Thiam, C. Antonelli, C. Iojoiu, F. Alloin, J.-Y. Sanchez, Optimizing ionic conduction of poly(oxyethylene) electrolytes through controlling the cross-link density, Electrochimica Acta, 240 (2017) 307-315.
[15] J. Mindemark, M.J. Lacey, T. Bowden, D. Brandell, Beyond PEO—Alternative host materials for Li+-conducting solid polymer electrolytes, Progress in Polymer Science, (2018).
[16] B. Sun, J. Mindemark, K. Edström, D. Brandell, Polycarbonate-based solid polymer electrolytes for Li-ion batteries, Solid State Ionics, 262 (2014) 738-742.
[17] Y. Tominaga, Ion-conductive polymer electrolytes based on poly(ethylene carbonate) and its derivatives, Polym J, 49 (2017) 291-299.
[18] J. Mindemark, B. Sun, E. Törmä, D. Brandell, High-performance solid polymer electrolytes for lithium batteries operational at ambient temperature, Journal of Power Sources, 298 (2015) 166-170.
[19] K. Kimura, J. Motomatsu, Y. Tominaga, Correlation between Solvation Structure and Ion-Conductive Behavior of Concentrated Poly(ethylene carbonate)-Based Electrolytes, The Journal of Physical Chemistry C, 120 (2016) 12385-12391.

[20] L. Meabe, N. Lago, L. Rubatat, C. Li, A.J. Müller, H. Sardon, M. Armand, D. Mecerreyes, Polycondensation as a Versatile Synthetic Route to Aliphatic Polycarbonates for Solid Polymer Electrolytes, Electrochimica Acta, 237 (2017) 259-266.
[21] J. Mindemark, L. Imholt, J. Montero, D. Brandell, Allyl ethers as combined plasticizing and crosslinkable side groups in polycarbonate-based polymer electrolytes for solid-state Li batteries, Journal of Polymer Science Part A: Polymer Chemistry, 54 (2016) 2128-2135.
[22] Y. Tominaga, V. Nanthana, D. Tohyama, Ionic conduction in poly(ethylene carbonate)-based rubbery electrolytes including lithium salts, Polym J, 44 (2012) 1155-1158.
[23] W. He, Z. Cui, X. Liu, Y. Cui, J. Chai, X. Zhou, Z. Liu, G. Cui, Carbonate-linked poly(ethylene oxide) polymer electrolytes towards high performance solid state lithium batteries, Electrochimica Acta, 225 (2017) 151-159.
[24] Y. Tominaga, K. Yamazaki, Fast Li-ion conduction in poly(ethylene carbonate)-based electrolytes and composites filled with TiO2 nanoparticles, Chemical Communications, 50 (2014) 4448-4450.
[25] J. Mindemark, A. Sobkowiak, G. Oltean, D. Brandell, T. Gustafsson, Mechanical Stabilization of Solid Polymer Electrolytes through Gamma Irradiation, Electrochimica Acta, 230 (2017) 189-195.
[26] L. Meabe, T.V. Huynh, N. Lago, H. Sardon, C. Li, L.A. O'Dell, M. Armand, M. Forsyth, D. Mecerreyes, Poly(ethylene oxide carbonates) solid polymer electrolytes for lithium batteries, Electrochimica Acta, 264 (2018) 367-375.
[27] L.I. Ronco, A. Basterretxea, D. Mantione, R.H. Aguirresarobe, R.J. Minari, L.M. Gugliotta, D. Mecerreyes, H. Sardon, Temperature responsive PEG-based polyurethanes “à la carte”, Polymer, 122 (2017) 117-124.
[28] L. Meabe, H. Sardon, D. Mecerreyes, Hydrolytically degradable poly(ethylene glycol) based polycarbonates by organocatalyzed condensation, European Polymer Journal, 95 (2017) 737-745.
[29] J. Evans, C.A. Vincent, P.G. Bruce, Electrochemical measurement of transference numbers in polymer electrolytes, Polymer, 28 (1987) 2324-2328.
[30] Y. Kato, S. Yokoyama, T. Yabe, H. Ikuta, Y. Uchimoto, M. Wakihara, Ionic conductivity and transport number of lithium ion in polymer electrolytes containing PEG–borate ester, Electrochimica Acta, 50 (2004) 281-284.
[31] G.B. Appetecchi, F. Alessandrini, R.G. Duan, A. Arzu, S. Passerini, Electrochemical testing of industrially produced PEO-based polymer electrolytes, Journal of Power Sources, 101 (2001) 42-46.